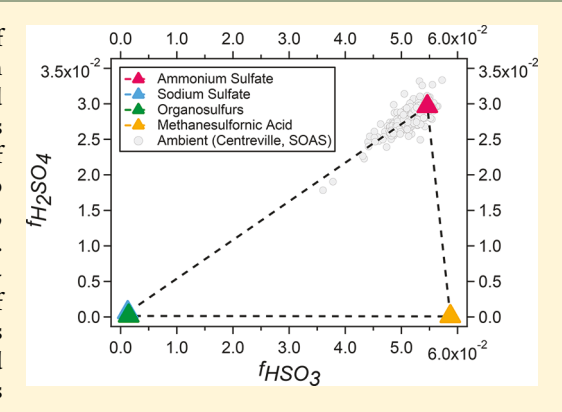


Response of the Aerodyne Aerosol Mass Spectrometer to Inorganic Sulfates and Organosulfur Compounds: Applications in Field and **Laboratory Measurements**

Yunle Chen, [†] Lu Xu, ^{‡,} [§] Tim Humphry, I Anusha P. S. Hettiyadura, ^{⊥,△} Jurgita Ovadnevaite, [#] Shan Huang, ^{∇,○} Laurent Poulain, I Jason C. Schroder, Pedro Campuzano-Jost, , I Pedro Campuzano-Jost, I Pedro Campu Jose L. Jimenez, ♣,¶® Hartmut Herrmann, O® Colin O'Dowd, Elizabeth A. Stone, L and Nga Lee Ng*,†,‡®

Supporting Information

ABSTRACT: Organosulfur compounds are important components of secondary organic aerosols (SOA). While the Aerodyne high-resolution time-of-flight aerosol mass spectrometer (AMS) has been extensively used in aerosol studies, the response of the AMS to organosulfur compounds is not well-understood. Here, we investigated the fragmentation patterns of organosulfurs and inorganic sulfates in the AMS, developed a method to deconvolve total sulfate into components of inorganic and organic origins, and applied this method in both laboratory and field measurements. Apportionment results from laboratory isoprene photooxidation experiment showed that with inorganic sulfate seed, sulfate functionality of organic origins can contribute ~7% of SOA mass at peak growth. Results from measurements in the Southeastern U.S. showed that 4% of measured sulfate is from organosulfur compounds. Methanesulfonic acid was estimated for measurements in the coastal and remote marine boundary



layer. We explored the application of this method to unit mass-resolution data, where it performed less well due to interferences. Our apportionment results demonstrate that organosulfur compounds could be a non-negligible source of sulfate fragments in AMS laboratory and field data sets. A reevaluation of previous AMS measurements over the full range of atmospheric conditions using this method could provide a global estimate/constraint on the contribution of organosulfur compounds.

INTRODUCTION

Organosulfur compounds have been identified in both laboratory-generated and ambient aerosols. 1-9 It has been suggested that these compounds can comprise a substantial fraction of organic aerosol (OA) mass. 3,6,9 Organosulfur compounds are generally of low volatility, 7,8 and can be an important component of high molecular weight (MW)

compounds in ambient aerosols. Due to their surface-active nature and chemical stability, 1,10,11 organosulfur compounds can play a potentially important role in altering aerosol

Received: February 11, 2019 Accepted: April 2, 2019 Published: April 2, 2019

[†]School of Earth and Atmospheric Sciences, Georgia Institute of Technology, Atlanta, Georgia 30332, United States

[‡]School of Chemical and Biomolecular Engineering, Georgia Institute of Technology, Atlanta, Georgia 30332, United States

[§]Now at Division of Geological and Planetary Sciences, California Institute of Technology, Pasadena, California 91125, United States

Department of Chemistry, Truman State University, Kirksville, Missouri 63501, United States

¹Department of Chemistry, University of Iowa, Iowa City, Iowa 52242, United States

^{*}School of Physics and Centre for Climate and Air Pollution Studies, Ryan Institute, National University of Ireland Galway, Galway H91 TK33, Ireland

 $^{^{}abla}$ Now at Institute for Environmental and Climate Research, Jinan University, Guangzhou, Guangdong 511443, China

^OLeibniz Institute for Tropospheric Research, Leipzig, Sachsen 04318, Germany

Department of Chemistry, University of Colorado, Boulder, Colorado 80309, United States

[¶]Cooperative Institute for Research in the Environmental Sciences (CIRES), University of Colorado, Boulder, Colorado 80309, United States

physicochemical properties. 5,12,13 Organosulfur compounds are also thought to be good tracers for aqueous secondary OA (SOA) formation. 14 Given their importance, different methods have been explored to quantify organosulfur compounds in ambient aerosols. Offline methods such as Fourier transform infrared (FT-IR) transmission spectroscopy have been used to measure C-O-S functional groups. 15 The difference between total particulate sulfur measured by X-ray emission techniques and water-soluble inorganic sulfate measured by ion chromatography (IC) has been used to provide an upperlimit estimation of atmospheric organosulfur compounds. 3,6,16,17 However, this method suffers uncertainties from instrument cross-calibrations. 17 Liquid chromatographyelectrospray ionization-tandem mass spectrometry (LC-ESI-MS/MS) is widely used to identify and quantify organosulfur compounds,5 but the quantification of total organosulfur compounds is limited by the availability of authentic standards. 10,18 For online methods, particle ablation by laser mass spectrometry (PALMS) single particle mass spectrometer has been used to measure certain organosulfur compounds in single particles, 9,19 but as a single particle mass spectrometer, PALMS suffers from quantification issues.²⁰

The high resolution time-of-flight aerosol mass spectrometer (HR-ToF-AMS, Aerodyne; henceforth referred to as AMS) has also been used to estimate the lower bound of ambient organosulfur compound concentrations based on the signal intensity of organosulfur ions $(C_xH_vO_zS^+)$ and their fractional contributions in pure organosulfur compound standards.²¹ However, most sulfate and sulfonate functionalities in organosulfur compounds fragment to $H_x SO_v^+$ ions. 21,22 Meanwhile, $H_xSO_y^+$ ions in the AMS are often misinterpreted as arising only from inorganic sulfates in subsequent analysis. This potential misattribution can result in an underestimation of organic mass and a corresponding overestimation of inorganic sulfate mass, and it also causes underestimation of S/C. Docherty et al.²³ have shown that when including the S content of organosulfates in elemental analysis calculations, S/ C can increase by a factor of 30 for an ambient study. Methanesulfonic acid, which is an important organosulfur compound in marine aerosols, ^{24,25} has been quantified with the AMS based on their signature organosulfur fragments (sometimes complemented by positive matrix factorization (PMF) analysis), 21,25-30 which are much more abundant due to the C-S bonding rather than C-O-S bonding, and the smaller size of methanesulfonic acid compared to other organosulfur compounds.31

In this study, we developed a method to estimate the concentration of organosulfur compounds based on AMSmeasured sulfate mass spectra. Sixteen standard organosulfur standards (including organosulfates, sulfonates, and sulfonic acids) were tested in the laboratory. Methanesulfonic acid was evaluated and discussed separately from other organosulfur compounds because of its distinctive mass spectrum. We applied this method to both chamber and ambient measurements and discussed their atmospheric implications. Four different AMSs were used in standard calibrations and chamber/ambient measurements, which will be referred hereafter as GT AMS (Georgia Institute of Technology group), Galway AMS (National University of Ireland Galway group), TROPOS AMS (Leibniz Institute for Tropospheric Research group), and Boulder AMS (University of Colorado-Boulder group) hereafter.

MATERIALS AND METHODS

Laboratory Characterization of Standard Compounds. The fragmentation patterns of standard compounds were obtained by directly atomizing 10-140 µM aqueous solutions of standard compounds into the AMS. The particles were generated by an ultrasonic nebulizer (U-5000AT, Cetac Technologies Inc., Omaha, NE), and passed through a nafion dryer to remove excess water prior to entering the AMS. In this study, three inorganic sulfates and sixteen organosulfur compounds were tested with the GT AMS (Supporting Information (SI) Table S2). The three inorganic sulfates are ammonium sulfate (AS), acidic AS (1:1 mixture of ammonium sulfate and sulfuric acid), and sodium sulfate (SS). The sixteen organosulfur compounds include four linear alkyl organosulfate salts (sodium methyl sulfate, sodium ethyl sulfate, sodium nheptyl sulfate, and sodium n-octyl sulfate), two oxygenated organosulfate salts, one containing a carboxylic acid functional group (potassium glycolic acid sulfate) and the other containing a carbonyl functional group (potassium hydroxyacetone sulfate), six aromatic organosulfate salts (potassium o-Cresol sulfate, potassium p-cresol sulfate, potassium m-cresol sulfate, sodium benzyl sulfate, potassium 4-nitrophenyl sulfate, and potassium 4-hydroxy-3-methoxyphenylglycol sulfate), two sulfonate salts (sodium 1-butanesulfonate and sodium benzenesulfonate), and two sulfonic acids (methanesulfonic acid and ethanesulfonic acid). Pure sulfuric acid mass spectrum was acquired with the Boulder AMS. Methanesulfonic acid (MSA) will be discussed separately from other organosulfur compounds due to its unique fragmentation patterns in the AMS. Organosulfate, sulfonate, and sulfonic acid standards tested in this study but excluding MSA will be referred to as OS hereafter.

Structures of standard compounds are shown in SI Table S2. Hydroxyacetone sulfate, glycolic acid sulfate, and benzyl sulfate were synthesized in the laboratory according to the method described in Hettiyadura et al.; o-cresol sulfate, p-cresol sulfate, and m-cresol sulfate were synthesized in the laboratory according to the method described in Staudt et al.; the rest of organosulfur standards are commercially available. Among all OS standards evaluated in this work, glycolic acid sulfate (OS-3) is one of the most abundant atmospheric organosulfates quantified so far. Hydroxyacetone sulfate (OS-4), methyl sulfate (OS-1), o-cresol sulfate (OS-7), p-cresol sulfate (OS-8), m-cresol sulfate (OS-9), and benzylsulfate (OS-10) have also been detected in ambient aerosols in prior studies.

Characterization of Chamber-Generated Biogenic SOA and Ambient OA. One isoprene photooxidation experiment under low-NO condition and four sets of field measurements conducted by different groups with different AMSs were investigated in this study to probe the time variations and abundance of organosulfur compounds in well-controlled single VOC system and in different ambient environments, including biogenic VOC (BVOC) dominated southeastern US measurements (Centreville SOAS measurements), MSA abundant coastal and cruise measurements (Mace Head and Polarstern measurements), and high acidity aircraft measurements (WINTER measurements). Details of the experiment and field measurements are presented in SI Section S1.

Four different AMS are included in the discussions, GT AMS (chamber isoprene SOA and Centreville measurements),

Galway AMS (Mace Head measurements), TROPOS AMS (Polarstern measurements), and Boulder AMS (WINTER measurements).

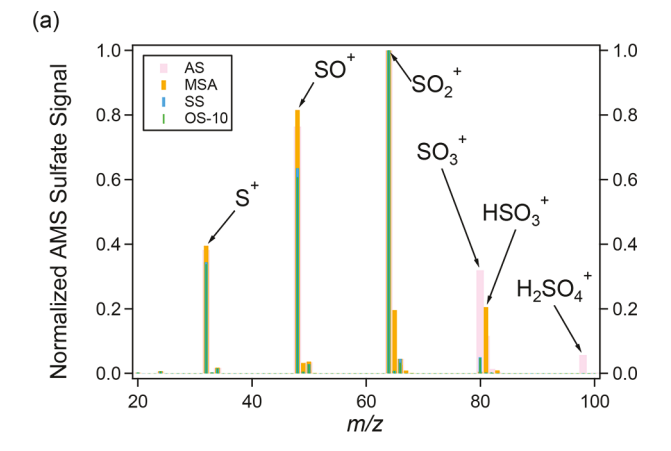
■ SULFATE APPORTIONMENT METHOD

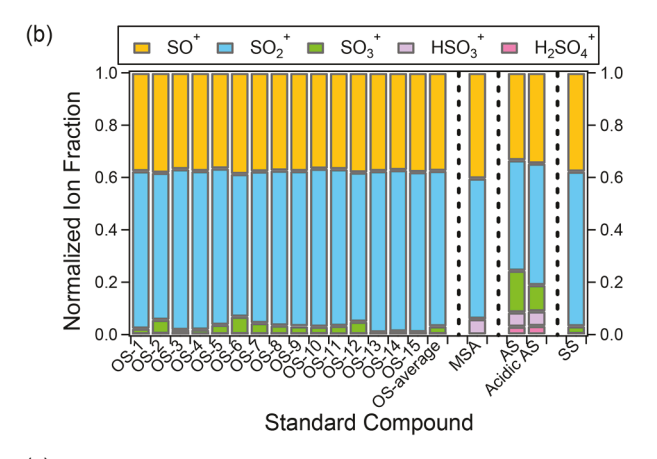
AMS Sulfate Mass Spectra of Standard Compounds.

Organosulfates, sulfonates, and sulfonic acids predominantly fragment into separate organic $(C_x H_v O_z^+)$ and sulfate fragments (H_xSO_y⁺) rather than organosulfur fragments $(C_xH_vO_zS^+)$ in the AMS (SI Figure S1), suggesting that most C-O-S (corresponding to organosulfates) and C-S (corresponding to sulfonates and sulfonic acids) bonds are not retained after vaporization and ionization. Sulfonate and sulfonic acid molecules do not contain a sulfate functional group, but the H_xSO_v fragments they produce in the AMS would be counted as sulfate concentrations in standard data processing. Therefore, these H_xSO_v fragments produced by sulfonates and sulfonic acids will still be referred to as "sulfate" fragments hereafter. For all OS tested in this study, organosulfur fragments only contribute 0.02-4% to the total signal, depending on the MW, structure, and bonding types (SI Figure S1). Generally, OS with smaller MW of carbon backbones tend to produce a larger fraction of organosulfur fragments, but the structure of the carbon backbones and bonding types may also play a role. For instance, methyl sulfate $(OS-1, H_3C-O-SO_3^-)$ and $MSA (H_3C-SO_3^-)$ have the same carbon backbone, but MSA retains a much higher portion of organosulfur fragments (16%) because of the different bond types between sulfate/sulfonate groups and the carbon backbones. This difference becomes negligible when one more methyl group is added to the carbon backbone (SI Figure S1, ethyl sulfate (OS-2) and ethanesulfonic acid (OS-15)). Phenyl sulfonates produce a higher fraction of organosulfur fragments compared to other OS with similar MW of carbon backbones (SI Figure S1, benzenesulfonate (OS-14)), possibly due to the stabilization by resonance between benzene ring and sulfonate group. 31 Due to their small signals, the organosulfur fragments are subject to interference by stronger neighboring signals in the most common V-mode resolution $(m/dm \sim 2500)$ for the AMS when sampling complex matrices such as ambient aerosols, posing a barrier to estimating OS mass only by organosulfur fragments. In contrast, the major sulfate fragments have strong signals and can be well fitted (SI Figures S2-S4). Consequently, we focused on using the sulfate fragments to understand the fragmentation patterns of different inorganic sulfates and organosulfur compounds in the AMS.

The typical V-mode AMS high-resolution sulfate mass spectra of AS, MSA, SS, and an OS standard (sodium benzyl sulfate, OS-10) are shown in Figure 1(a). The spectra obtained in this study show a very similar pattern to those reported elsewhere. Among all the sulfate fragments produced by the fragmentation of these different sulfate/sulfonate-containing compounds, the main ions are SO⁺, SO₂⁺, SO₃⁺, HSO₃⁺, and $\text{H}_2\text{SO}_4^{+}$. Here, we referred to the sum of these five ions as Σ HSO and normalized each of the five ions to Σ HSO. The normalization can be expressed by eqs 1–6.

The normalized SO^+ , SO_2^+ , SO_3^+ , HSO_3^+ , and $H_2SO_4^+$ abundance is shown in Figure 1(b). For all standards, smaller ions like SO^+ , SO_2^+ and SO_3^+ account for most of the ΣHSO signals, which can be explained by the extensive thermal decomposition during vaporization and fragmentation after electron impact (EI) ionization. Meanwhile, the HSO_3^+ fragment is only produced by MSA and AS (at different





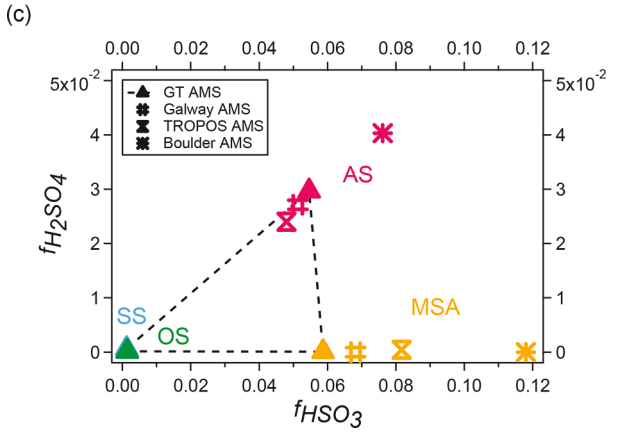


Figure 1. (a) Typical normalized sulfate mass spectra of organosulfur compounds (OS; OS-10 refers to sodium benzyl sulfate in SI Table S2), ammonium sulfate (AS), methanesulfonic acid (MSA), and sodium sulfate (SS), not including water fragments. (b) Mass fraction of five selected HSO ions. (c) $f_{\rm H_2SO_4}$ vs. $f_{\rm HSO_3}$ for standard compounds. For OS, the shown $f_{\rm HSO_3}$ and $f_{\rm H_2SO_4}$ are averages for all fifteen OS. OS and SS standard calibrations were only performed with the GT AMS, whereas MSA and AS standard calibrations were performed with multiple AMSs.

relative abundances), and $\rm H_2SO_4^+$ fragment is exclusively produced by AS. These observations can be explained by their different chemical structures. For organosulfates, it takes less energy to break the O–S bond than the C–O bond, ³⁶ so it is more likely for the organic part to retain the oxygen during fragmentation and result in small sulfate fragments with at most three oxygens. For MSA, the sulfur molecule is bonded to

three oxygens so that the H₂SO₄⁺ ion cannot be produced, whereas the HSO₃⁺ ion can be produced by breaking the C-S bond. For ammonium sulfate, sulfate either decomposes to dehydrated SO_3 (+H₂O) or evaporates as intact H₂SO₄, ³⁷ and the water signal produced due to the dehydration process is calculated based on an empirical sulfate fragmentation table (SI Table S4).³⁷ For the other sulfate/sulfonate-containing species discussed in this study (MSA, OS, and SS), there is no pathway to produce water fragments, therefore a sulfate fragmentation table without water fragments was used for these species (SI Table S4).

$$\sum HSO = SO^{+} + SO_{2}^{+} + SO_{3}^{+} + HSO_{3}^{+} + H_{2}SO_{4}^{+}$$
 (1)

$$f_{SO} = \frac{SO^{+}}{\sum HSO}$$
 (2)

$$f_{SO_2} = \frac{SO_2^+}{\sum HSO} \tag{3}$$

$$f_{SO_3} = \frac{SO_3^+}{\sum HSO} \tag{4}$$

$$f_{\text{HSO}_3} = \frac{\text{HSO}_3^+}{\sum \text{HSO}} \tag{5}$$

$$f_{\rm H_2SO_4} = \frac{{\rm H_2SO_4}^+}{\sum {\rm HSO}} \tag{6}$$

The distinctive HSO_3^+ and $H_2SO_4^+$ ion fractions in different standard compounds provide the basis for our method of distinguishing different types of sulfate/sulfonate-containing compounds. Figure 1(c) shows the $f_{\rm H_2SO_4}$ vs. $f_{\rm HSO_3}$ for all standard compounds. The four types of standards (AS, OS, SS, and MSA) together define a triangle-shaped space, with OS and SS occupying indistinguishable regions in this space. There are some variations in f_{HSO_3} and $f_{H_2SO_4}$ among all OS (SI Table S3), but the variations are small, thus the average value for all OS will be used hereafter. Different types of inorganic sulfates and organosulfur compounds fall into different regions in this space and thus can be distinguished. The relative contribution from each type of sulfate/sulfonate-containing compounds can be estimated for any point in this space. The mass spectra of AS and MSA obtained by the Galway AMS, TROPOS AMS, and Boulder AMS are also shown in Figure 1(c). The differences in the same type of compounds among different AMSs likely arise from instrument-to-instrument and time-totime variability. Therefore, when applying the apportionment method, calibrations with SS/OS, AS, and MSA standards to define the triangle region are required for the particular instrument and time period. In addition, calibrations of RIE (relative ionization efficiency of the species of interest relative to nitrate)³⁵ for the standard species are required for accurate quantification.

Development of Sulfate Apportionment Method.

Based on the different f_{HSO_3} and $_{H_2SO_4}$ for different types of sulfate/sulfonate-containing compounds, we developed an approach to deconvolve total sulfate signals into components of inorganic and organic origins. Based on the $f_{\rm HSO_2}$ and $f_{\rm HsSO_4}$ values determined for pure standard compounds in the laboratory, the measured HSO₃⁺, H₂SO₄⁺, and ∑HSO can be expressed as

$$\begin{split} & \text{HSO}_{3,\text{meas}} = f_{\text{HSO}_3,\text{AS},\text{standard}} \times \sum \text{HSO}_{\text{AS}} + f_{\text{HSO}_3,\text{OS/SS},\text{standard}} \\ & \times \sum \text{HSO}_{\text{OS/SS}} + f_{\text{HSO}_3,\text{MSA},\text{standard}} \times \sum \text{HSO}_{\text{MSA}} \end{aligned} \tag{7}$$

$$\begin{split} &\mathbf{H}_{2}\mathbf{SO}_{4,\text{meas}} = f_{\mathbf{H}_{2}\mathbf{SO}_{4},\mathbf{AS},\text{standard}} \times \mathbf{\Sigma}\mathbf{HSO}_{\mathbf{AS}} + f_{\mathbf{H}_{2}\mathbf{SO}_{4},\mathbf{OS}/\mathbf{SS},\text{standard}} \\ &\times \mathbf{\Sigma}\mathbf{HSO}_{\mathbf{OS/SS}} + f_{\mathbf{H}_{3}\mathbf{SO}_{4},\mathbf{MSA},\text{standard}} \times \mathbf{\Sigma}\mathbf{HSO}_{\mathbf{MSA}} \end{aligned} \tag{8}$$

$$\Sigma HSO_{\text{meas}} = \Sigma HSO_{\text{AS}} + \Sigma HSO_{\text{OS/SS}} + \Sigma HSO_{\text{MSA}}$$
 (9)

The subscript "meas" denotes the measured mass concentration of sulfate fragments, and the subscript "standard" denotes measured fractions of standard compounds. ΣHSO_{AS} , Σ HSO_{OS/SS}, and Σ HSO_{MSA} are Σ HSO for AS, OS or SS, and MSA, respectively, which can be solved by eq 10.

Afterwards, the fractions of \sum HSO in AMS total sulfate signals (i.e., $\left(\frac{\sum_{HSO}}{total sulfate}\right)_{standard}$) acquired for each type of compounds during the calibrations will be used to convert \sum HSO signals from above calculations to total sulfate signals.

For OS and SS, they are indistinguishable in the $f_{H_2SO_4}$ vs. $f_{\rm HSO_3}$ space, but their relative contributions to total sulfate in ambient data can be highly dependent on the measurement locations. SS is considered as a refractory species and cannot be completely vaporized at 600 °C (default AMS vaporizer temperature).³⁸ As a result, for typical continental sites, SS signals may be a minor component compared to OS. For coastal and cruise measurements, SS cannot be neglected due to its abundance. In the following discussion, we will treat Yellowith The Section 1 Section 2 Property of the Yellowith Sectin dominantly from OS (except for a short period of crustal events), and for coastal or marine measurements (Mace Head and Polarstern), we will treat OS and SS as one component, that is, the summation of OS and SS.

Laboratory Calibration of Sulfate RIE. The sulfate RIE in the AMS (RIE_{SO4}) can be calibrated with pure ammonium sulfate.³⁹ The default RIE_{SO4} of 1.2 was used for ammonium sulfate in this study because this calibration was not performed for the majority of the field studies discussed here. Our twoyear records (2017-2018) of RIE_{SO4} on the GT AMS is 1.20 \pm 0.15, validating that 1.2 is a good estimation. The RIE_{SO4} of organosulfate compounds can be lower than that of ammonium sulfate, since during the fragmentation and ionization processes, the electronegative sulfate/sulfonate groups have a reduced tendency to retain the charge. 23,40,41

$$\begin{bmatrix} \boldsymbol{\Sigma} \boldsymbol{H} \boldsymbol{S} \boldsymbol{O}_{AS} \\ \boldsymbol{\Sigma} \boldsymbol{H} \boldsymbol{S} \boldsymbol{O}_{OS/SS} \\ \boldsymbol{\Sigma} \boldsymbol{H} \boldsymbol{S} \boldsymbol{O}_{MSA} \end{bmatrix} = \begin{bmatrix} f_{\boldsymbol{H} \boldsymbol{S} \boldsymbol{O}_{3}, \boldsymbol{AS}, \boldsymbol{s} \boldsymbol{t} \boldsymbol{a} \boldsymbol{n} \boldsymbol{d} \boldsymbol{d}} & f_{\boldsymbol{H} \boldsymbol{S} \boldsymbol{O}_{3}, \boldsymbol{OS}/SS, \boldsymbol{s} \boldsymbol{t} \boldsymbol{a} \boldsymbol{n} \boldsymbol{d} \boldsymbol{d}} & f_{\boldsymbol{H} \boldsymbol{S} \boldsymbol{O}_{3}, \boldsymbol{MS} \boldsymbol{A}, \boldsymbol{s} \boldsymbol{t} \boldsymbol{a} \boldsymbol{n} \boldsymbol{d} \boldsymbol{d}} \\ f_{\boldsymbol{H}_{2} \boldsymbol{S} \boldsymbol{O}_{4}, \boldsymbol{AS}, \boldsymbol{s} \boldsymbol{t} \boldsymbol{a} \boldsymbol{n} \boldsymbol{d} \boldsymbol{d}} & f_{\boldsymbol{H}_{2} \boldsymbol{S} \boldsymbol{O}_{4}, \boldsymbol{OS}/SS, \boldsymbol{s} \boldsymbol{t} \boldsymbol{a} \boldsymbol{n} \boldsymbol{d} \boldsymbol{d}} & f_{\boldsymbol{H}_{2} \boldsymbol{S} \boldsymbol{O}_{4}, \boldsymbol{MS} \boldsymbol{A}, \boldsymbol{s} \boldsymbol{t} \boldsymbol{a} \boldsymbol{n} \boldsymbol{d} \boldsymbol{d}} \\ 1 & 1 & 1 & 1 \end{bmatrix}^{-1} \begin{bmatrix} \boldsymbol{H} \boldsymbol{S} \boldsymbol{O}_{3, \boldsymbol{m} \boldsymbol{e} \boldsymbol{a} \boldsymbol{s}} \\ \boldsymbol{H}_{2} \boldsymbol{S} \boldsymbol{O}_{4, \boldsymbol{m} \boldsymbol{e} \boldsymbol{a} \boldsymbol{s}} \\ \boldsymbol{\Sigma} \boldsymbol{H} \boldsymbol{S} \boldsymbol{O}_{4, \boldsymbol{m} \boldsymbol{e} \boldsymbol{a} \boldsymbol{s}} \end{bmatrix}$$

$$(10)$$

The RIE_{SO4} was determined for two commercially available organosulfur compounds (MSA and ethyl sodium sulfate (OS-2)) with the GT AMS. Size-selected (300 nm) pure MSA (or OS-2) was atomized to the AMS and a condensation particle counter (CPC; TSI 3775) simultaneously. Sulfate concentration based on particle number was calculated by

$$[SO_4]_{CPC} = \frac{n_{CPC}\pi\rho D_p^3}{6} f_{SO_4, \text{formula}}$$
(11)

where n_{CPC} is the particle number concentration measured by CPC, ρ is the density of organosulfur compounds, $D_{\rm p}$ is the selected particle diameter, and $f_{SO4,formula}$ is the sulfate functionality mass fraction according to the compound formula (e.g., 81/96 for MSA). The collection efficiency (CE) of 1 was applied to AMS data. Viscosity measurements of organosulfur compounds are lacking in literature. Here we assumed that MSA and OS-2 particles are of low viscosity given their low MW, 42,43 while uncertainty regarding this assumption exits. An RIE_{SO4} of 0.77 was calculated for MSA and an RIE_{SO4} of 0.82 was calculated for OS-2 (SI Figure S5). The reason for the lower RIE_{SO4} for MSA is because a higher fraction of organosulfur fragments was produced in the fragmentation process of MSA compared to OS-2 (SI Figure S1), and these fragments were not accounted in the sulfate concentration in eq 11. For the subsequent analysis, we tentatively applied an RIE of 0.8 to sulfate produced by organosulfur compounds. A default RIE of 1.2 was applied to "AS sulfate".

RESULTS AND DISCUSSION

Sulfate Apportionment for Laboratory-Generated Binary Mixtures. The sulfate apportionment method was first validated with laboratory-generated aerosols of known compositions. Two different types of standard compound solutions were premixed and nebulized into an AMS (GT AMS). Particles with a mobility diameter of 300 nm were selected.

We first tested the mixture of AS with MSA. MSA and AS were dissolved in deionized (DI) water in different molar ratios (3:1, 2:1, 1:1, 1:2, 1:3). The mixture solution was immediately nebulized into the AMS. After obtaining Σ HSO_{MSA} and Σ HSO_{AS} by eq 10, total sulfate signals by MSA ("MSA sulfate") and AS ("AS sulfate") were calculated by

$$SO_{4,MSA} = \frac{\sum HSO_{MSA}}{RIE_{SO4,MSA}} \left(\frac{\sum HSO}{SO_4}\right)_{MSA, standard}$$
(12)

$$SO_{4,AS} = \frac{\sum HSO_{AS}}{RIE_{SO4,AS}} \left(\frac{\sum HSO}{SO_4}\right)_{AS, standard}$$
(13)

SI Figure S6(a) shows "MSA sulfate" to "AS sulfate" molar ratio calculated by apportionment method as a function of MSA to AS molar ratio in the particles. The MSA to AS ratio in the particles was assumed to be the same as that in the solution. 44–46 MW of 98 g/mol and 81 g/mol are used for "AS sulfate" and "MSA sulfate", respectively, to calculate their molar ratios. The calculated "MSA sulfate" to "AS sulfate" ratio agreed well with particle compositions (slope = 0.97 \pm 0.02).

A similar binary mixture apportionment analysis was carried out for mixtures of AS with an OS standard. The results of AS and ethanesulfonic acid (OS-15) mixtures are shown in SI Figure S6(b). Similarly, the calculated sulfate produced by OS ("OS sulfate") to "AS sulfate" ratio is highly correlated with

particle composition. The slope is lower than 1 (0.88 \pm 0.04) but still within the uncertainty of AMS measurements.

Effect of Particle Acidity on AS Fragmentation Pattern. Considering marine and stratospheric aerosols are rich in sulfuric acid, 2S,47 and the particle pH is low in the southeastern U.S., 48 we investigated the fragmentation pattern of acidic AS. Acidic sulfate (1:1 mixture of ammonium sulfate and sulfuric acid) was tested with the GT AMS, and pure sulfuric acid was tested with the Boulder AMS. The results are shown in Figure 2(a). All $f_{\rm HSO_3}$ and $f_{\rm H_3SO_4}$ are normalized to

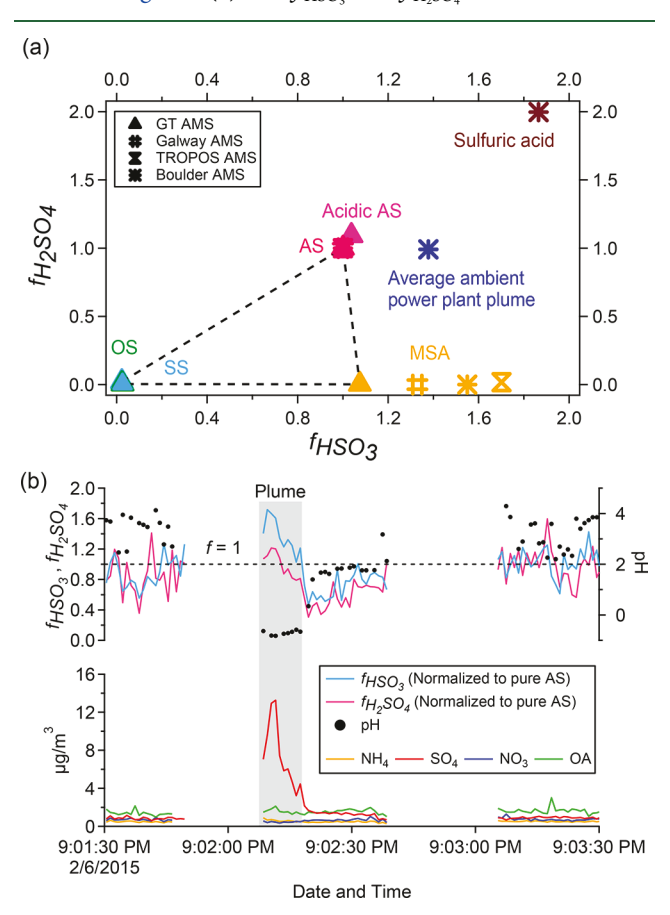


Figure 2. (a) $f_{\rm H_2SO_4}$ vs. $f_{\rm HSO_3}$ for standard compounds and the strong SO₂ plume (average data) during the WINTER aircraft campaign. Both $f_{\rm HSO_3}$ and $f_{\rm H_2SO_4}$ are normalized to those of AS from the specific AMS, so that AS would always be at (1,1) (b) Evolution of $f_{\rm HSO_3}$ and $f_{\rm H_2SO_4}$ (normalized to pure AS), pH, and AMS species in a power plant plume in WINTER aircraft campaign. Acidic AS is 1:1 mixture of ammonium sulfate and sulfuric acid.

those of AS from the specific AMS to minimize the influence from instrument-to-instrument variability, so that AS would always be at point (1,1) in the $f_{\rm H2SO4}$ vs. $f_{\rm HSO3}$ space. Acidic AS shows a similar fragmentation pattern to AS, with a slightly higher production of ${\rm HSO_3}^+$ and ${\rm H_2SO_4}^+$ fragments (SI Table S3 and Figure 2(a)). However, pure sulfuric acid shows almost twice higher fractions of ${\rm HSO_3}^+$ and ${\rm H_2SO_4}^+$ fragments (Figure 2 (a)) compared to AS. We speculate that the reason is that a much larger fraction evaporates intact for pure sulfuric acid, compared to the fraction of the sulfate that evaporates as sulfuric acid for AS and acidic AS, and dehydration is more likely to happen for sulfate salts than sulfuric acid. 37,49 Since vaporization equilibrium between ${\rm H_2SO_4}$ and ${\rm SO_3} + {\rm H_2O}$ can

shift with changing temperature, a precise temperature control of the AMS vaporizer and a MS tuning that favors a non massdependent response are necessary.³⁹

The Boulder AMS was also deployed in the WINTER aircraft campaign, 50 where it intercepted a strong coal-fired power plant plume (\sim 50 ppb SO₂). As shown in Figure 2(b), the estimated particle pH (calculated with the E-AIM model⁵¹⁻⁵³) decreased rapidly to -1 in the core of the plume. The highest f_{HSO_3} and f_{H,SO_4} values in the plume are 72% and 21% higher, respectively, compared to pure AS from the same AMS. In this strong plume, the sulfate concentration is an order of magnitude higher than ammonium, nitrate, and organics concentrations, thus the change in f_{HSO} , and f_{HsSO} is attributed to the near sulfuric acid conditions and very high acidity. The shifts in $f_{\rm HSO_3}$ and $f_{\rm H_2SO_4}$ to values outside the region defined by the OS/SS-AS-MSA triangle suggest that caution is needed when applying the apportionment method to data obtained under high acidity (near pure H2SO4 molar ratio of NH₄:SO₄< 0.8) conditions. Nevertheless, for ground studies the ambient particles are less acidic than pure sulfuric acid particles in most cases.^{54–58}

Sulfate Apportionment for Chamber-Generated Isoprene SOA. Organosulfates can be formed in isoprene photooxidation reactions.^{2,59} Here, we applied the sulfate apportionment method to quantify OS formation in an isoprene photooxidation experiment. 60 The reaction profile is shown in Figure 3. The increase in total sulfate concentration

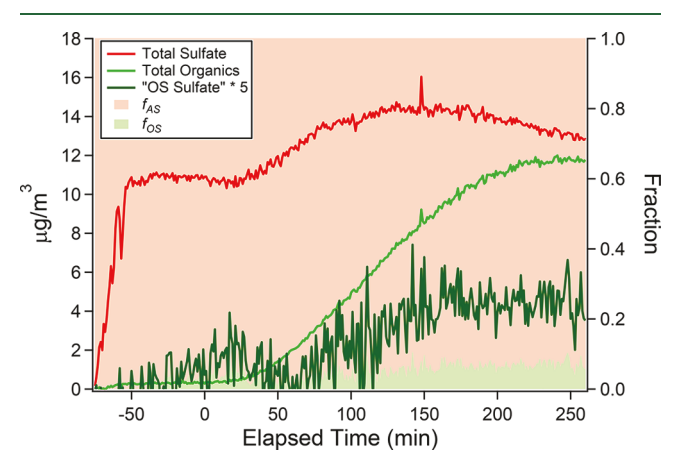


Figure 3. Reaction profile of the chamber isoprene photooxidation experiment. The f_{AS} and f_{OS} refer to fraction of "AS sulfate" and "OS sulfate", respectively, in total sulfate.

as SOA started to form is likely due to increase in CE with the condensation of organics.^{61,62} We assumed all O-S bonds in C-O-S structures (corresponding to organosulfates) are broken. Thus, no organosulfur fragments are produced, and sulfate/sulfonate functionality MW is 80 g/mol (corresponding to SO₃) for all OS. With these, we estimated that 7% of AS seed has become organosulfate as SOA reaches peak growth, and the "OS sulfate" could contribute to 7% of total SOA. C_xH_vO_zS⁺ ions only account for 0.07% of total SOA, consolidating our assumption that almost all O-S bonds in C-O-S structures are broken to form "OS sulfate". Prior studies have shown that the formation of isoprene-epoxydiol (IEPOX) organosulfate (one of the abundant isoprene-derived organonsulfates) is strongly enhanced in the presence of acidic sulfate seed. 2,59,63-66 As our chamber experiment was conducted under dry conditions with ammonium sulfate seed, the contribution of organosulfates to total organic aerosols is expected to be lower than those under humid acidic

Application to Field Measurements for OS Estimation. We applied the sulfate apportionment method to the SOAS data⁶⁹ from Centreville to deconvolve sulfate from AS, OS, and MSA, respectively. The average "OS sulfate" mass is $0.12 \mu g/m^3$ for the whole campaign, which means that 4% of measured sulfate is from OS. We note that there are some negative values (6% of all the data) in the calculated "OS sulfate" concentration, which is due to data points falling outside the AS-MSA line in the triangle (SI Figure S7(a)), as expected due to measurement noise. Our apportionment result is consistent with recent airborne and ground measurements in the same region. Liao et al. quantified IEPOX-sulfate using PALMS during flight measurements and determined that it accounted for ~5% of the total sulfate mass measured by AMS.9 Hu et al. also indicated that IEPOX-sulfate accounted for ~5% of total sulfate mass for SOAS measurements. 67 Previous study by Guo et al. 48 showed that AMS total sulfate is 20% higher than inorganic sulfate measured by particle-intoliquid-sampler coupled to an ion chromatograph (PILS-IC) during SOAS. After excluding the OS sulfate calculated from our apportionment method, the resulting AMS "AS sulfate" shows a better agreement (slope = 0.97) with PM₁ inorganic sulfate measured by PILS-IC (Figure 4(a)).

We also compare our OS with speciated organosulfur compounds quantified in PM_{2.5} filter samples collected at Centreville during SOAS, using offline hydrophilic interaction liquid chromatography (HILIC) and a triple quadrupole mass spectrometer (TQD MS) against authentic standards.⁶⁸ We focus on OS compounds that are both used in the apportionment method development in this study and quantified in the filter analysis. The "OS sulfate" time series calculated by sulfate apportionment method is shown in Figure 4(b), together with total sulfate measured by the AMS, 70,71 methyl sulfate, glycolic acid sulfate and hydroxyacetone sulfate quantitatively measured by offline HILIC-TQD,68 and isoprene-OA resolved by PMF. 70,71 The AMS "OS sulfate" shows a moderate correlation (R = 0.52) with speciated organosulfur compounds measured by offline HILIC-TQD. Two periods 6/17/2013-6/18/2013 and 6/24/2013-6/28/ 2013 are excluded when calculating the R value, because these two periods overlap with the crustal events when mineral cations are abundant and the contribution of SS is not negligible.⁷² For the "OS sulfate" spike on 6/26/2013, we speculated that it is due to the overlap of crustal event with strong isoprene-related OS formation. Further, we compared "OS sulfate" with AMS isoprene-OA factor under different isoprene-OA abundances to study the role of isoprene-derived OS at Centreville. As shown in Figure 4(c), the correlation between "OS sulfate" and isoprene-OA is enhanced as the fraction of isoprene-OA in total OA increases. The improved correlation between "OS sulfate" and isoprene-OA as isoprene-OA fraction increases is consistent with isoprene-derived OS being an important source of OS at Centreville in summer when isoprene is abundant.⁶⁸ Such enhancement in correlation is not observed for other OA factors (SI Figure S8), suggesting that even if other factors may contribute to OS, they are not

A recent new study characterized twelve types of organosulfur compounds in filter samples of PM_{2.5} collected from **Environmental Science & Technology**

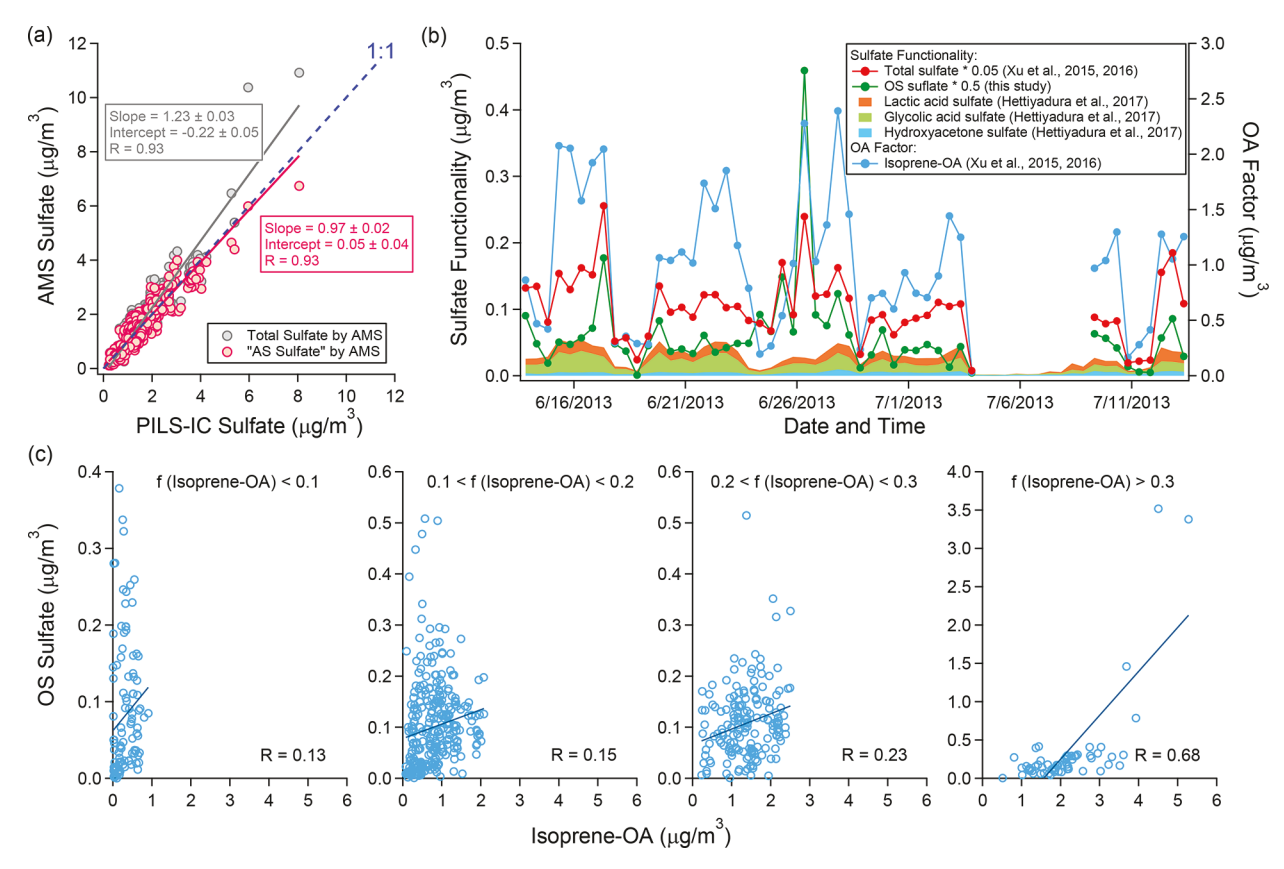


Figure 4. (a) Comparison of AMS total sulfate and AMS "AS sulfate" (calculated by sulfate apportionment method) with PM₁ inorganic sulfate (measured by PILS-IC). (b) Time series of total sulfate (measured by the AMS), "OS sulfate" (calculated by sulfate apportionment method), sulfate functionality concentration of main organosulfur compounds (measured by offline HILIC-TQD), and isoprene-OA factor (resolved by PMF). (c) Comparison of "OS sulfate" with isoprene-OA. The Pearson's R is obtained by linear least-squares fit.

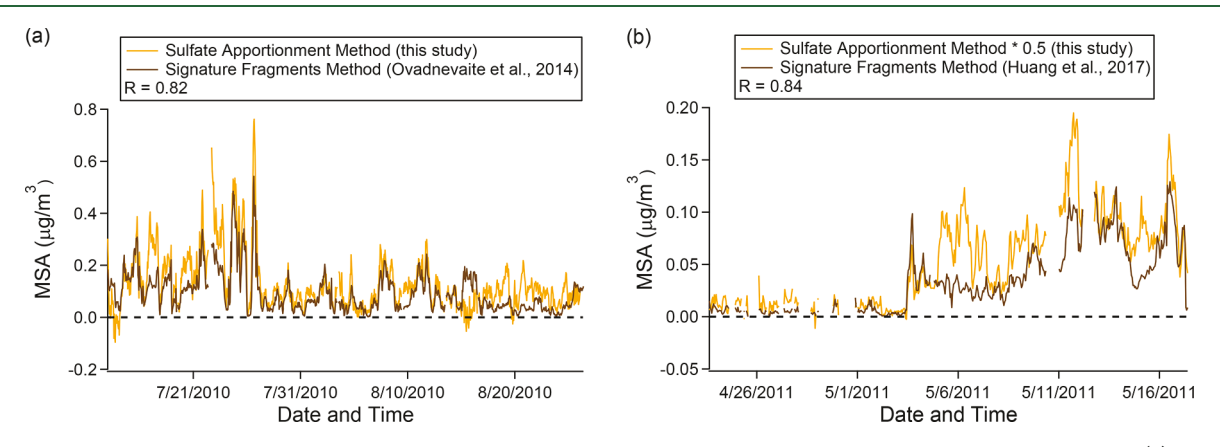


Figure 5. Comparison of MSA mass concentration estimated by sulfate apportionment method and signature fragments method for (a) Mace Head measurements and (b) Polarstern measurements. The Pearson's *R* is obtained by linear least-squares fit.

SOAS. The sulfate mass associated with these twelve organosulfates over the studied period averaged 0.37 $\mu g/m^3$, with 2-methyltetrol sulfate accounting for 80% of the "OS sulfate" mass. These filter results imply that total "OS sulfate" could account for 16% of the total sulfate mass, which is higher than our estimation and prior studies by Liao et al. and Hu et al. Two instruments measuring particles of different sizes (PM₁ by the AMS and PM_{2.5} by filter) and uncertainties in different instrument/measurement techniques likely contribute to the different observations. In this study, we cannot exclude the possibility that the fragmentation pattern of 2-methyltetrol sulfate in the AMS is different from other OS standards. Future

work is warranted to expand the analysis to encompass an even wider suite of OS standards as they become available and characterize OS sulfate measured by different techniques.

Application to Field Measurements for MSA Estimation. For measurements at coastal sites (Mace Head measurements) and from cruises (*R/V Polarstern* measurements), we focused on resolving MSA time variations, in a similar manner to OS estimation, using 96 g/mol as MSA MW and 81 g/mol as sulfonic acid functionality MW.

Previous studies have reported the quantification of MSA with the AMS by a well-developed signature fragments method based on ions such as CH_3SO_2^+ , CH_4SO_3^+ , etc., $^{21,25-29}_{}$ which

are almost solely produced by MSA. Based on the fragmentation pattern of the pure MSA standard, ambient MSA concentration can be calculated using the intensity of signature fragments and their relative contributions in pure MSA. Here, we compared MSA concentration calculated by the signature fragments method and sulfate apportionment method presented in this study. The results for Mace Head and the R/V Polarstern measurements are shown in Figure 5. For both data sets, the MSA concentration estimated by the two methods shows good correlation (R = 0.82 for Mace Head data, and R = 0.84 for Polarstern data). Compared to the signature fragments method, the average concentration estimated by sulfate apportionment method is higher by 30% for Mace Head measurements and 150% for Polarstern measurements. The reason is currently unknown, but a possible cause could be that the high acidity of submicron marine aerosols^{74,75} affects sulfate fragmentation pattern as discussed above. For instance, for the Polarstern measurements, even accounting for the presence of large amount of sea salt sulfate, most data points have higher fractions of HSO₃⁺ and H₂SO₄⁺ fragments than the AS standard (SI Figure S7(c)). Meanwhile, some data points fall outside the OS/SS-AS line in the triangle (SI Figure S7(b), (c)), resulting in negative concentrations in MSA estimation (Figure 5), which requires further investigation. Nevertheless, this shows that the sulfate apportionment method is capable of determining the presence of MSA and its approximate concentration, and of approximately separating the MSA contribution from that of AS and OS species.

Implications. In this study, a novel sulfate apportionment method was developed for AMS analysis. We showed that sulfate fragments originated from organosulfur compounds can be resolved from those of inorganic sulfate based on their different sulfate fragmentation patterns, providing insights into the quantity and time variations of organosulfur compounds in the atmosphere. The advantage of this method is that the contribution of "AS sulfate", "OS/SS sulfate", and "MSA sulfate" can be directly estimated using AMS measurements with high time resolution. One thing to note is that the sulfate apportionment method only estimates the mass concentration of sulfate/sulfonate functionalities in organosulfur molecules. The estimation of total OS contribution depends on the estimation of OS MW.

We note that there are several limitations of this study. First, while we have considered an extensive set of atmospherically relevant OS standards, given the variety and complexity of atmospherically relevant organosulfur compounds, additional standards should be evaluated to explore the robustness of the fragmentation patterns of organosulfur compounds presented here. Second, we found that the sulfate fragmentation pattern can be very different under high acidity, making this method not directly applicable under near sulfuric acid conditions, though such extreme particle acidity is not common in typical continental surface measurements. Third, when data points fall outside the triangular region defined by OS/SS-AS-MSA, the estimated concentrations (either OS/SS, AS, or MSA, depending on where the data point falls) could be negative. As this will always occur to some degree due to the impact of random noise, averaging of longer data periods may be more meaningful under low concentration conditions.

Currently, the AMS sulfate is often misinterpreted as being entirely inorganic sulfate. Here, we applied the sulfate apportionment method to both chamber and ambient measurements. Our apportionment results clearly demonstrate that organosulfur compounds could be a non-negligible source of sulfate fragments in the AMS. Future studies need to take this into account when reporting organic and inorganic mass concentrations from AMS measurements. In addition to high-resolution (HR) analysis, we also explored the plausibility of deconvolving AMS sulfate for unit mass resolution (UMR) measurements in the SI Section S3. Overall, quantitative measurements of organosulfur compounds with high time-resolution will allow for improved constraints of their abundance in different environments and help advance the understanding of organosulfur compounds formation and related chemical processes in the atmosphere.

ASSOCIATED CONTENT

S Supporting Information

The Supporting Information is available free of charge on the ACS Publications website at DOI: 10.1021/acs.est.9b00884.

Brief descriptions of uncertainty analysis and UMR analysis, details of standard compounds characterization, and supplementary figures (PDF)

AUTHOR INFORMATION

Corresponding Author

*E-mail: ng@chbe.gatech.edu.

ORCID ®

Yunle Chen: 0000-0001-9904-2638 Lu Xu: 0000-0002-0021-9876 Shan Huang: 0000-0001-5575-4510

Pedro Campuzano-Jost: 0000-0003-3930-010X

Jose L. Jimenez: 0000-0001-6203-1847 Hartmut Herrmann: 0000-0001-7044-2101 Nga Lee Ng: 0000-0001-8460-4765

Present Address

△A.P.S.H.: Department of Chemistry, Purdue University, West Lafayette, Indiana 47907, United States

Notes

The authors declare no competing financial interest.

■ ACKNOWLEDGMENTS

This research was supported by NSF AGS-1455588 and U.S. Environmental Protection Agency STAR grant RD-83540301. We thank Dan Dan Huang and Chak K. Chan for helpful discussions. E.A.S., A.P.S.H., and T. H. were supported by EPA STAR grant 83540101. The measurements and data analysis at Centreville were supported by NSF AGS-1242258 and EPA RD-83540301. The measurements and data analysis at Mace Head were supported by the Horizon 2020 research and innovation programme ACTRIS-2 Integrating Activities (grant agreement No. 654109) and EPA-Ireland (AEROSOURCE, 2016-CCRP-MS-31). The measurements on board R/VPolarstern were supported by Polarstern expedition AWI_ANT XXVII/4, and the data analysis was supported by Gottfried Wilhelm Leibniz Association (OCEANET project in the framework of PAKT). J.C.S., P.C.J., and J.L.J. acknowledge funding from NSF AGS-1822664 and NASA NNX15AT96G. This publication's contents are solely the responsibility of the grantee and do not necessarily represent the official views of the US EPA. Further, U.S. EPA does not endorse the purchase of any commercial products or services mentioned in the publication.

REFERENCES

- (1) Liggio, J.; Li, S.-M. Organosulfate formation during the uptake of pinonaldehyde on acidic sulfate aerosols. *Geophys. Res. Lett.* **2006**, 33 (13), L13808.
- (2) Surratt, J. D.; Kroll, J. H.; Kleindienst, T. E.; Edney, E. O.; Claeys, M.; Sorooshian, A.; Ng, N. L.; Offenberg, J. H.; Lewandowski, M.; Jaoui, M.; Flagan, R. C.; Seinfeld, J. H. Evidence for Organosulfates in Secondary Organic Aerosol. *Environ. Sci. Technol.* 2007, 41 (2), 517–527.
- (3) Surratt, J. D.; Gómez-González, Y.; Chan, A. W. H.; Vermeylen, R.; Shahgholi, M.; Kleindienst, T. E.; Edney, E. O.; Offenberg, J. H.; Lewandowski, M.; Jaoui, M.; Maenhaut, W.; Claeys, M.; Flagan, R. C.; Seinfeld, J. H. Organosulfate Formation in Biogenic Secondary Organic Aerosol. *J. Phys. Chem. A* **2008**, *112* (36), 8345–8378.
- (4) Riva, M.; Tomaz, S.; Cui, T.; Lin, Y.-H.; Perraudin, E.; Gold, A.; Stone, E. A.; Villenave, E.; Surratt, J. D. Evidence for an Unrecognized Secondary Anthropogenic Source of Organosulfates and Sulfonates: Gas-Phase Oxidation of Polycyclic Aromatic Hydrocarbons in the Presence of Sulfate Aerosol. *Environ. Sci. Technol.* **2015**, 49 (11), 6654–6664.
- (5) Stone, E. A.; Yang, L.; Yu, L. E.; Rupakheti, M. Characterization of organosulfates in atmospheric aerosols at Four Asian locations. *Atmos. Environ.* **2012**, *47*, 323–329.
- (6) Tolocka, M. P.; Turpin, B. Contribution of Organosulfur Compounds to Organic Aerosol Mass. *Environ. Sci. Technol.* **2012**, *46* (15), 7978–7983.
- (7) Iinuma, Y.; Müller, C.; Böge, O.; Gnauk, T.; Herrmann, H. The formation of organic sulfate esters in the limonene ozonolysis secondary organic aerosol (SOA) under acidic conditions. *Atmos. Environ.* **2007**, *41* (27), 5571–5583.
- (8) Iinuma, Y.; Müller, C.; Berndt, T.; Böge, O.; Claeys, M.; Herrmann, H. Evidence for the Existence of Organosulfates from β -Pinene Ozonolysis in Ambient Secondary Organic Aerosol. *Environ. Sci. Technol.* **2007**, 41 (19), 6678–6683.
- (9) Liao, J.; Froyd, K. D.; Murphy, D. M.; Keutsch, F. N.; Yu, G.; Wennberg, P. O.; St. Clair, J. M.; Crounse, J. D.; Wisthaler, A.; Mikoviny, T.; Jimenez, J. L.; Campuzano-Jost, P.; Day, D. A.; Hu, W.; Ryerson, T. B.; Pollack, I. B.; Peischl, J.; Anderson, B. E.; Ziemba, L. D.; Blake, D. R.; Meinardi, S.; Diskin, G. Airborne measurements of organosulfates over the continental U.S. *Journal of Geophysical Research: Atmospheres.* 2015, 120 (7), 2990–3005.
- (10) Olson, C. N.; Galloway, M. M.; Yu, G.; Hedman, C. J.; Lockett, M. R.; Yoon, T.; Stone, E. A.; Smith, L. M.; Keutsch, F. N. Hydroxycarboxylic Acid-Derived Organosulfates: Synthesis, Stability, and Quantification in Ambient Aerosol. *Environ. Sci. Technol.* **2011**, 45 (15), 6468–6474.
- (11) Darer, A. I.; Cole-Filipiak, N. C.; O'Connor, A. E.; Elrod, M. J. Formation and Stability of Atmospherically Relevant Isoprene-Derived Organosulfates and Organonitrates. *Environ. Sci. Technol.* **2011**, 45 (5), 1895–1902.
- (12) Tao, S.; Lu, X.; Levac, N.; Bateman, A. P.; Nguyen, T. B.; Bones, D. L.; Nizkorodov, S. A.; Laskin, J.; Laskin, A.; Yang, X. Molecular Characterization of Organosulfates in Organic Aerosols from Shanghai and Los Angeles Urban Areas by Nanospray-Desorption Electrospray Ionization High-Resolution Mass Spectrometry. *Environ. Sci. Technol.* **2014**, *48* (18), 10993–11001.
- (13) Estillore, A. D.; Hettiyadura, A. P. S.; Qin, Z.; Leckrone, E.; Wombacher, B.; Humphry, T.; Stone, E. A.; Grassian, V. H. Water Uptake and Hygroscopic Growth of Organosulfate Aerosol. *Environ. Sci. Technol.* **2016**, *50* (8), 4259–4268.
- (14) McNeill, V. F.; Woo, J. L.; Kim, D. D.; Schwier, A. N.; Wannell, N. J.; Sumner, A. J.; Barakat, J. M. Aqueous-Phase Secondary Organic Aerosol and Organosulfate Formation in Atmospheric Aerosols: A Modeling Study. *Environ. Sci. Technol.* **2012**, *46* (15), 8075–8081.
- (15) Maria, S. F.; Russell, L. M.; Turpin, B. J.; Porcja, R. J.; Campos, T. L.; Weber, R. J.; Huebert, B. J. Source signatures of carbon monoxide and organic functional groups in Asian Pacific Regional Aerosol Characterization Experiment (ACE-Asia) submicron aerosol types. *J. Geophys. Res.* **2003**, *108* (D23), n/a-n/a.

- (16) Sorooshian, A.; Crosbie, E.; Maudlin, L. C.; Youn, J.-S.; Wang, Z.; Shingler, T.; Ortega, A. M.; Hersey, S.; Woods, R. K. Surface and Airborne Measurements of Organosulfur and Methanesulfonate Over the Western United States and Coastal Areas. *Journal of geophysical research*. *Atmospheres: JGR.* **2015**, *120* (16), 8535–8548.
- (17) Lukács, H.; Gelencsér, A.; Hoffer, A.; Kiss, G.; Horváth, K.; Hartyáni, Z. Quantitative assessment of organosulfates in size-segregated rural fine aerosol. *Atmos. Chem. Phys.* **2009**, 9 (1), 231–238.
- (18) Hettiyadura, A. P. S.; Stone, E. A.; Kundu, S.; Baker, Z.; Geddes, E.; Richards, K.; Humphry, T. Determination of atmospheric organosulfates using HILIC chromatography with MS detection. *Atmos. Meas. Tech.* **2015**, 8 (6), 2347–2358.
- (19) Froyd, K. D.; Murphy, S. M.; Murphy, D. M.; de Gouw, J. A.; Eddingsaas, N. C.; Wennberg, P. O. Contribution of isoprene-derived organosulfates to free tropospheric aerosol mass. *Proc. Natl. Acad. Sci. U. S. A.* **2010**, *107* (50), 21360–21365.
- (20) Murphy, D. M. The design of single particle laser mass spectrometers. *Mass Spectrom. Rev.* **2007**, 26 (2), 150–165.
- (21) Huang, D. D.; Li, Y. J.; Lee, B. P.; Chan, C. K. Analysis of Organic Sulfur Compounds in Atmospheric Aerosols at the HKUST Supersite in Hong Kong Using HR-ToF-AMS. *Environ. Sci. Technol.* **2015**, 49 (6), 3672–3679.
- (22) Farmer, D. K.; Matsunaga, A.; Docherty, K. S.; Surratt, J. D.; Seinfeld, J. H.; Ziemann, P. J.; Jimenez, J. L. Response of an aerosol mass spectrometer to organonitrates and organosulfates and implications for atmospheric chemistry. *Proc. Natl. Acad. Sci. U. S. A.* 2010, 107 (15), 6670–6675.
- (23) Docherty, K. S.; Aiken, A. C.; Huffman, J. A.; Ulbrich, I. M.; DeCarlo, P. F.; Sueper, D.; Worsnop, D. R.; Snyder, D. C.; Peltier, R. E.; Weber, R. J.; Grover, B. D.; Eatough, D. J.; Williams, B. J.; Goldstein, A. H.; Ziemann, P. J.; Jimenez, J. L. The 2005 Study of Organic Aerosols at Riverside (SOAR-1): instrumental intercomparisons and fine particle composition. *Atmos. Chem. Phys.* 2011, 11 (23), 12387–12420.
- (24) Facchini, M. C.; Decesari, S.; Rinaldi, M.; Carbone, C.; Finessi, E.; Mircea, M.; Fuzzi, S.; Moretti, F.; Tagliavini, E.; Ceburnis, D.; O'Dowd, C. D. Important Source of Marine Secondary Organic Aerosol from Biogenic Amines. *Environ. Sci. Technol.* **2008**, 42 (24), 9116–9121.
- (25) Ovadnevaite, J.; Ceburnis, D.; Leinert, S.; Dall'Osto, M.; Canagaratna, M.; O'Doherty, S.; Berresheim, H.; O'Dowd, C. Submicron NE Atlantic marine aerosol chemical composition and abundance: Seasonal trends and air mass categorization. *Journal of Geophysical Research: Atmospheres.* **2014**, *119* (20), 11 850–11,863.
- (26) Phinney, L.; Richard Leaitch, W.; Lohmann, U.; Boudries, H.; Worsnop, D. R.; Jayne, J. T.; Toom-Sauntry, D.; Wadleigh, M.; Sharma, S.; Shantz, N. Characterization of the aerosol over the subarctic north east Pacific Ocean. *Deep Sea Res., Part II* **2006**, *53* (20–22), 2410–2433.
- (27) Zorn, S. R.; Drewnick, F.; Schott, M.; Hoffmann, T.; Borrmann, S. Characterization of the South Atlantic marine boundary layer aerosol using an aerodyne aerosol mass spectrometer. *Atmos. Chem. Phys.* **2008**, 8 (16), 4711–4728.
- (28) Ge, X.; Zhang, Q.; Sun, Y.; Ruehl, C. R.; Setyan, A. Effect of aqueous-phase processing on aerosol chemistry and size distributions in Fresno, California, during wintertime. *Environmental Chemistry*. **2012**, *9* (3), 221–235.
- (29) Huang, S.; Poulain, L.; van Pinxteren, D.; van Pinxteren, M.; Wu, Z.; Herrmann, H.; Wiedensohler, A. Latitudinal and Seasonal Distribution of Particulate MSA over the Atlantic using a Validated Quantification Method with HR-ToF-AMS. *Environ. Sci. Technol.* **2017**, *51* (1), 418–426.
- (30) Willis, M. D.; Burkart, J.; Thomas, J. L.; Kollner, F.; Schneider, J.; Bozem, H.; Hoor, P. M.; Aliabadi, A. A.; Schulz, H.; Herber, A. B.; Leaitch, W. R.; Abbatt, J. P. D. Growth of nucleation mode particles in the summertime Arctic: a case study. *Atmos. Chem. Phys.* **2016**, *16* (12), 7663–7679.

- (31) Oae, S. Organic Sulfur Chemistry: Structure and Mechanism; CRC Press: Boca Raton, FL, 1991.
- (32) Staudt, S.; Kundu, S.; Lehmler, H.-J.; He, X.; Cui, T.; Lin, Y.-H.; Kristensen, K.; Glasius, M.; Zhang, X.; Weber, R. J.; Surratt, J. D.; Stone, E. A. Aromatic organosulfates in atmospheric aerosols: Synthesis, characterization, and abundance. *Atmos. Environ.* **2014**, 94, 366–373.
- (33) Huang, R. J.; Cao, J. J.; Chen, Y.; Yang, L.; Shen, J. C.; You, Q. H.; Wang, K.; Lin, C. S.; Xu, W.; Gao, B.; Li, Y. J.; Chen, Q.; Hoffmann, T.; O'Dowd, C. D.; Bilde, M.; Glasius, M. Organosulfates in atmospheric aerosol: synthesis and quantitative analysis of PM2.5 from Xi'an, northwestern China. *Atmos. Meas. Tech.* **2018**, *11* (6), 3447–3456.
- (34) Hogrefe, O.; Drewnick, F.; Lala, G. G.; Schwab, J. J.; Demerjian, K. L. Development, operation and applications of an aerosol generation, calibration and research facility. *Aerosol Sci. Technol.* **2004**, 38, 196–214.
- (35) Canagaratna, M.; Jayne, J.; Jimenez, J.; Allan, J.; Alfarra, M.; Zhang, Q.; Onasch, T.; Drewnick, F.; Coe, H.; Middlebrook, A. Chemical and microphysical characterization of ambient aerosols with the aerodyne aerosol mass spectrometer. *Mass Spectrom. Rev.* **2007**, 26 (2), 185–222.
- (36) Sanderson, R. T. Chemical Bonds and Bond Energy; Academic Press: New York, 1971.
- (37) Allan, J. D.; Delia, A. E.; Coe, H.; Bower, K. N.; Alfarra, M. R.; Jimenez, J. L.; Middlebrook, A. M.; Drewnick, F.; Onasch, T. B.; Canagaratna, M. R.; Jayne, J. T.; Worsnop, D. R. A generalised method for the extraction of chemically resolved mass spectra from Aerodyne aerosol mass spectrometer data. *J. Aerosol Sci.* **2004**, *35* (7), 909–922
- (38) Allan, J. D.; Bower, K. N.; Coe, H.; Boudries, H.; Jayne, J. T.; Canagaratna, M. R.; Millet, D. B.; Goldstein, A. H.; Quinn, P. K.; Weber, R. J.; Worsnop, D. R. Submicron aerosol composition at Trinidad Head, California, during ITCT 2K2: Its relationship with gas phase volatile organic carbon and assessment of instrument performance. *Journal of Geophysical Research: Atmospheres.* **2004**, 109 (D23), n/a-n/a.
- (39) Hu, W.; Campuzano-Jost, P.; Day, D. A.; Croteau, P.; Canagaratna, M. R.; Jayne, J. T.; Worsnop, D. R.; Jimenez, J. L. Evaluation of the new capture vapourizer for aerosol mass spectrometers (AMS) through laboratory studies of inorganic species. *Atmos. Meas. Tech.* **2017**, *10* (8), 2897–2921.
- (40) Aiken, A. C.; DeCarlo, P. F.; Jimenez, J. L. Elemental Analysis of Organic Species with Electron Ionization High-Resolution Mass Spectrometry. *Anal. Chem.* **2007**, *79* (21), 8350–8358.
- (41) Aiken, A. C.; DeCarlo, P. F.; Kroll, J. H.; Worsnop, D. R.; Huffman, J. A.; Docherty, K. S.; Ulbrich, I. M.; Mohr, C.; Kimmel, J. R.; Sueper, D.; Sun, Y.; Zhang, Q.; Trimborn, A.; Northway, M.; Ziemann, P. J.; Canagaratna, M. R.; Onasch, T. B.; Alfarra, M. R.; Prevot, A. S. H.; Dommen, J.; Duplissy, J.; Metzger, A.; Baltensperger, U.; Jimenez, J. L. O/C and OM/OC Ratios of Primary, Secondary, and Ambient Organic Aerosols with High-Resolution Time-of-Flight Aerosol Mass Spectrometry. *Environ. Sci. Technol.* 2008, 42 (12), 4478–4485.
- (42) Shiraiwa, M.; Li, Y.; Tsimpidi, A. P.; Karydis, V. A.; Berkemeier, T.; Pandis, S. N.; Lelieveld, J.; Koop, T.; Poschl, U. Global distribution of particle phase state in atmospheric secondary organic aerosols. *Nat. Commun.* **2017**, *8*, 7.
- (43) DeRieux, W. S. W.; Li, Y.; Lin, P.; Laskin, J.; Laskin, A.; Bertram, A. K.; Nizkorodov, S. A.; Shiraiwa, M. Predicting the glass transition temperature and viscosity of secondary organic material using molecular composition. *Atmos. Chem. Phys.* **2018**, *18* (9), 6331–6351.
- (44) Matthew, B. M.; Middlebrook, A. M.; Onasch, T. B. Collection Efficiencies in an Aerodyne Aerosol Mass Spectrometer as a Function of Particle Phase for Laboratory Generated Aerosols. *Aerosol Sci. Technol.* **2008**, 42 (11), 884–898.
- (45) Xu, W.; Croteau, P.; Williams, L.; Canagaratna, M.; Onasch, T.; Cross, E.; Zhang, X.; Robinson, W.; Worsnop, D.; Jayne, J. Laboratory

- characterization of an aerosol chemical speciation monitor with PM2.5 measurement capability. *Aerosol Sci. Technol.* **2017**, *51* (1), 69–83.
- (46) Xu, W.; Lambe, A.; Silva, P.; Hu, W.; Onasch, T.; Williams, L.; Croteau, P.; Zhang, X.; Renbaum-Wolff, L.; Fortner, E.; Jimenez, J. L.; Jayne, J.; Worsnop, D.; Canagaratna, M. Laboratory evaluation of species-dependent relative ionization efficiencies in the Aerodyne Aerosol Mass Spectrometer. *Aerosol Sci. Technol.* **2018**, 52 (6), 626–641.
- (47) Murphy, D. M.; Cziczo, D. J.; Hudson, P. K.; Thomson, D. S. Carbonaceous material in aerosol particles in the lower stratosphere and tropopause region. *J. Geophys. Res.* **2007**, *112*, D4.
- (48) Guo, H.; Xu, L.; Bougiatioti, A.; Cerully, K. M.; Capps, S. L.; Hite Jr, J. R.; Carlton, A. G.; Lee, S. H.; Bergin, M. H.; Ng, N. L.; Nenes, A.; Weber, R. J. Fine-particle water and pH in the southeastern United States. *Atmos. Chem. Phys.* **2015**, *15* (9), 5211–5228.
- (49) Drewnick, F.; Diesch, J. M.; Faber, P.; Borrmann, S. Aerosol mass spectrometry: particle-vaporizer interactions and their consequences for the measurements. *Atmos. Meas. Tech.* **2015**, *8* (9), 3811–3830.
- (50) Schroder, J. C.; Campuzano-Jost, P.; Day, D. A.; Shah, V.; Larson, K.; Sommers, J. M.; Sullivan, A. P.; Campos, T.; Reeves, J. M.; Hills, A.; Hornbrook, R. S.; Blake, N. J.; Scheuer, E.; Guo, H.; Fibiger, D. L.; McDuffie, E. E.; Hayes, P. L.; Weber, R. J.; Dibb, J. E.; Apel, E. C.; Jaeglé, L.; Brown, S. S.; Thornton, J. A.; Jimenez, J. L. Sources and Secondary Production of Organic Aerosols in the Northeastern United States during WINTER. *Journal of Geophysical Research: Atmospheres.* 2018, 123 (14), 7771–7796.
- (51) Clegg, S. L.; Brimblecombe, P.; Wexler, A. S. Thermodynamic model of the system H+-NH₄⁺-SO₄²-NO₃⁻-H₂O at tropospheric temperatures. *J. Phys. Chem. A* **1998**, *102* (12), 2137–2154.
- (52) Wexler, A. S.; Clegg, S. L. Atmospheric aerosol models for systems including the ions H^+ , NH_4^+ , Na^+ , $SO_4^{\ 2^-}$, NO_3^- , Cl^- , Br^- , and H_2O . *J. Geophys. Re., Atmos.* **2002**, *107* (D14), 14.
- (53) Clegg, S. L.; Seinfeld, J. H.; Edney, E. O. Thermodynamic modelling of aqueous aerosols containing electrolytes and dissolved organic compounds. II. An extended Zdanovskii-Stokes-Robinson approach. J. Aerosol Sci. 2003, 34 (6), 667–690.
- (54) Zhang, Q.; Jimenez, J. L.; Worsnop, D. R.; Canagaratna, M. A Case Study of Urban Particle Acidity and Its Influence on Secondary Organic Aerosol. *Environ. Sci. Technol.* **2007**, *41* (9), 3213–3219.
- (55) Bougiatioti, A.; Nikolaou, P.; Stavroulas, I.; Kouvarakis, G.; Weber, R.; Nenes, A.; Kanakidou, M.; Mihalopoulos, N. Particle water and pH in the eastern Mediterranean: source variability and implications for nutrient availability. *Atmos. Chem. Phys.* **2016**, *16* (7), 4579–4591.
- (56) Guo, H.; Weber, R. J.; Nenes, A. High levels of ammonia do not raise fine particle pH sufficiently to yield nitrogen oxide-dominated sulfate production. *Sci. Rep.* **2017**, *7* (1), 12109.
- (57) Liu, M.; Song, Y.; Zhou, T.; Xu, Z.; Yan, C.; Zheng, M.; Wu, Z.; Hu, M.; Wu, Y.; Zhu, T. Fine particle pH during severe haze episodes in northern China. *Geophys. Res. Lett.* **2017**, 44 (10), 5213–5221.
- (58) Guo, H.; Liu, J.; Froyd, K. D.; Roberts, J. M.; Veres, P. R.; Hayes, P. L.; Jimenez, J. L.; Nenes, A.; Weber, R. J. Fine particle pH and gas—particle phase partitioning of inorganic species in Pasadena, California, during the 2010 CalNex campaign. *Atmos. Chem. Phys.* 2017, 17 (9), 5703–5719.
- (59) Surratt, J. D.; Chan, A. W.; Eddingsaas, N. C.; Chan, M.; Loza, C. L.; Kwan, A. J.; Hersey, S. P.; Flagan, R. C.; Wennberg, P. O.; Seinfeld, J. H. Reactive intermediates revealed in secondary organic aerosol formation from isoprene. *Proc. Natl. Acad. Sci. U. S. A.* **2010**, 107 (15), 6640–6645.
- (60) Tuet, W. Y.; Chen, Y.; Xu, L.; Fok, S.; Gao, D.; Weber, R. J.; Ng, N. L. Chemical oxidative potential of secondary organic aerosol (SOA) generated from the photooxidation of biogenic and anthropogenic volatile organic compounds. *Atmos. Chem. Phys.* **2017**, *17* (2), 839–853.
- (61) Docherty, K. S.; Jaoui, M.; Corse, E.; Jimenez, J. L.; Offenberg, J. H.; Lewandowski, M.; Kleindienst, T. E. Collection Efficiency of the

- Aerosol Mass Spectrometer for Chamber-Generated Secondary Organic Aerosols. Aerosol Sci. Technol. 2013, 47 (3), 294-309.
- (62) Bahreini, R.; Keywood, M. D.; Ng, N. L.; Varutbangkul, V.; Gao, S.; Flagan, R. C.; Seinfeld, J. H.; Worsnop, D. R.; Jimenez, J. L. Measurements of Secondary Organic Aerosol from Oxidation of Cycloalkenes, Terpenes, and m-Xylene Using an Aerodyne Aerosol Mass Spectrometer. *Environ. Sci. Technol.* **2005**, *39* (15), 5674–5688.
- (63) Lin, Y.-H.; Zhang, Z.; Docherty, K. S.; Zhang, H.; Budisulistiorini, S. H.; Rubitschun, C. L.; Shaw, S. L.; Knipping, E. M.; Edgerton, E. S.; Kleindienst, T. E.; Gold, A.; Surratt, J. D. Isoprene Epoxydiols as Precursors to Secondary Organic Aerosol Formation: Acid-Catalyzed Reactive Uptake Studies with Authentic Compounds. *Environ. Sci. Technol.* **2012**, *46* (1), 250–258.
- (64) Riedel, T. P.; Lin, Y. H.; Zhang, Z.; Chu, K.; Thornton, J. A.; Vizuete, W.; Gold, A.; Surratt, J. D. Constraining condensed-phase formation kinetics of secondary organic aerosol components from isoprene epoxydiols. *Atmos. Chem. Phys.* **2016**, *16* (3), 1245–1254.
- (65) Zhang, Y.; Chen, Y.; Lambe, A. T.; Olson, N. E.; Lei, Z.; Craig, R. L.; Zhang, Z.; Gold, A.; Onasch, T. B.; Jayne, J. T.; Worsnop, D. R.; Gaston, C. J.; Thornton, J. A.; Vizuete, W.; Ault, A. P.; Surratt, J. D. Effect of the Aerosol-Phase State on Secondary Organic Aerosol Formation from the Reactive Uptake of Isoprene-Derived Epoxydiols (IEPOX). *Environ. Sci. Technol. Lett.* 2018, 5 (3), 167–174.
- (66) Cui, T.; Zeng, Z.; dos Santos, E. O.; Zhang, Z.; Chen, Y.; Zhang, Y.; Rose, C. A.; Budisulistiorini, S. H.; Collins, L. B.; Bodnar, W. M.; de Souza, R. A. F.; Martin, S. T.; Machado, C. M. D.; Turpin, B. J.; Gold, A.; Ault, A. P.; Surratt, J. D. Development of a hydrophilic interaction liquid chromatography (HILIC) method for the chemical characterization of water-soluble isoprene epoxydiol (IEPOX)-derived secondary organic aerosol. *Environmental Science: Processes & Impacts.* 2018, 20 (11), 1524–1536.
- (67) Hu, W. W.; Campuzano-Jost, P.; Palm, B. B.; Day, D. A.; Ortega, A. M.; Hayes, P. L.; Krechmer, J. E.; Chen, Q.; Kuwata, M.; Liu, Y. J.; de Sá, S. S.; McKinney, K.; Martin, S. T.; Hu, M.; Budisulistiorini, S. H.; Riva, M.; Surratt, J. D.; St. Clair, J. M.; Isaacman-Van Wertz, G.; Yee, L. D.; Goldstein, A. H.; Carbone, S.; Brito, J.; Artaxo, P.; de Gouw, J. A.; Koss, A.; Wisthaler, A.; Mikoviny, T.; Karl, T.; Kaser, L.; Jud, W.; Hansel, A.; Docherty, K. S.; Alexander, M. L.; Robinson, N. H.; Coe, H.; Allan, J. D.; Canagaratna, M. R.; Paulot, F.; Jimenez, J. L. Characterization of a real-time tracer for isoprene epoxydiols-derived secondary organic aerosol (IEPOX-SOA) from aerosol mass spectrometer measurements. *Atmos. Chem. Phys.* 2015, 15 (20), 11807–11833.
- (68) Hettiyadura, A. P. S.; Jayarathne, T.; Baumann, K.; Goldstein, A. H.; de Gouw, J. A.; Koss, A.; Keutsch, F. N.; Skog, K.; Stone, E. A. Qualitative and quantitative analysis of atmospheric organosulfates in Centreville, Alabama. *Atmos. Chem. Phys.* **2017**, *17* (2), 1343–1359. (69) Xu, L.; Guo, H.; Boyd, C. M.; Klein, M.; et al. Effects of anthropogenic emissions on aerosol formation from isoprene and
- (69) Xu, L.; Guo, H.; Boyd, C. M.; Klein, M.; et al. Effects of anthropogenic emissions on aerosol formation from isoprene and monoterpenes in the southeastern United States. *Proc. Natl. Acad. Sci. U. S. A.* **2015**, *112*, 37–42.
- (70) Xu, L.; Guo, H.; Boyd, C. M.; Klein, M.; Bougiatioti, A.; Cerully, K. M.; Hite, J. R.; Isaacman-VanWertz, G.; Kreisberg, N. M.; Knote, C.; Olson, K.; Koss, A.; Goldstein, A. H.; Hering, S. V.; de Gouw, J.; Baumann, K.; Lee, S. H.; Nenes, A.; Weber, R. J.; Ng, N. L. Effects of anthropogenic emissions on aerosol formation from isoprene and monoterpenes in the southeastern United States. *Proc. Natl. Acad. Sci. U. S. A.* 2015, 112 (1), 37–42.
- (71) Xu, L.; Suresh, S.; Guo, H.; Weber, R. J.; Ng, N. L. Aerosol characterization over the southeastern United States using high-resolution aerosol mass spectrometry: spatial and seasonal variation of aerosol composition and sources with a focus on organic nitrates. *Atmos. Chem. Phys.* **2015**, *15* (13), 7307–7336.
- (72) Allen, H. M.; Draper, D. C.; Ayres, B. R.; Ault, A.; Bondy, A.; Takahama, S.; Modini, R. L.; Baumann, K.; Edgerton, E.; Knote, C.; Laskin, A.; Wang, B.; Fry, J. L. Influence of crustal dust and sea spray supermicron particle concentrations and acidity on inorganic NO₃⁻ aerosol during the 2013 Southern Oxidant and Aerosol Study. *Atmos. Chem. Phys.* **2015**, *15* (18), 10669–10685.

- (73) Hettiyadura, A. P. S.; Xu, L.; Jayarathne, T.; Skog, K.; Guo, H.; Weber, R. J.; Nenes, A.; Keutsch, F. N.; Ng, N. L.; Stone, E. A. Source apportionment of organic carbon in Centreville, AL using organosulfates in organic tracer-based positive matrix factorization. *Atmos. Environ.* **2018**, *186*, 74–88.
- (74) Fridlind, A. M.; Jacobson, M. Z. A study of gas-aerosol equilibrium and aerosol pH in the remote marine boundary layer during the First Aerosol Characterization Experiment (ACE 1). *Journal of Geophysical Research: Atmospheres.* **2000**, *105* (D13), 17325–17340.
- (75) Keene, W. C.; Pszenny, A. A. P.; Maben, J. R.; Stevenson, E.; Wall, A. Closure evaluation of size-resolved aerosol pH in the New England coastal atmosphere during summer. *Journal of Geophysical Research: Atmospheres.* **2004**, *109* (D23), n/a-n/a.